Experimental and Theoretical Studies on Tautomerism and Acid−Base Behavior of *N*-(2-Oxo-2*H*-chromen-3-yl)acetamide

Cemil Öğretir,*,† Murat Duran,† and Sinem Aydemir‡

Department of Chemistry and Department of Physics, Faculty of Arts & Sciences, Eskişehir Osmangazi University, 26480 Eskişehir, Turkey

The structures of all of the chemical species involved in the prototropic tautomerism and acid−base dissociation equilibria of *N*-(2-oxo-2*H*-chromen-3-yl)acetamide were determined both experimentally and theoretically. Using the calculated acidity constants, the prototropic equilibrium constants for keto−enol tautomerizm were determined. The enolate and the keto-amino forms were found to be predominant. The gauge including atomic orbital method for calculating ^{1}H and ^{13}C NMR nuclear magnetic shielding tensors at both the Hartree−Fock and density functional levels of theory was applied to *N*-(2-oxo-2*H*-chromen-3-yl)acetamide. The obtained theoretical data were compared to the experimental data. A satisfactory agreement between the experimental chemical shifts and the theoretical values of shielding constants were obtained. Acceptable correlations were presented between experimental and theoretical results.

Introduction

The coumarin system is present in a very broad range of natural and non-natural products of biological interest.[1] Coumarin derivatives are important naturally occurring and synthetic compounds which show several relevant applications. In particular, they exhibit different biological activities, including anticoagulant, spasmolytic, diuretic, anthelmintic, and hypoglucemic actions.[2−9] In the present study, we focused our attention on *N*-(2-oxo-2*H*-chromen-3-yl)acetamide (3-acetamidocoumarin; 3AC) which is a substituted coumarin bearing a relatively volumous substituent at position 3 of the α-pyrone ring.

The acidity constant, pK_a, of a compound is an important property in both the life sciences and in chemistry.[10] The most important of the parameters are lipohilicity, solubility, permeability, and apparent acid dissociaton constants (K_a), because these factors determine the absorption and bioavailability of the molecule.[11−14] The K_a value is an important parameter to estimate the extent of ionization of drug molecules at different pH values, which is of fundamental importance in the consideration of their interaction with biological membranes and in their synthesis.[15,16] The ability to cross the blood−brain barrier toward the site of action can be characterized by some physicochemical parameters, such as acidity constants, pK_a, which can predict the behavior of biologically active compounds in living organisms governing their ionization degree at the physiological pH value.[17] Following our work on drug precursor 2-amino-4-(3 or 4-substituted phenyl)thiazole derivatives,[18] we now report on the acid−base and tautomeric behavior of 3AC (Figure 1).

* To whom correspondence should be addressed. Tel: +90 222 239 37 50/2873. Fax: +90 222 239 35 78. E-mail: cogretir@ogu.edu.tr.
† Department of Chemistry.
‡ Department of Physics.

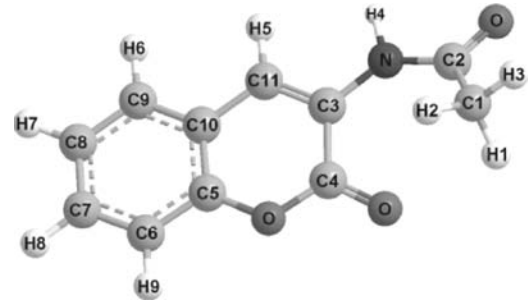

Figure 1. Atomic numeration of 3AC.

Experimental Section

Reagents. The structure of 3AC is depicted in Figure 1. The reagent (98%) was obtained from Sigma-Aldrich and was used without further purification. The other reagents were of analytical grade.

Materials and Solutions. The buffer solutions employed were prepared from (a) HCl−KCl, pH 1; (b) KH_2PO_4−NaOH, pH 7.0; (c) Borax−HCl, pH 8.0−9.0; (d) Borax−NaOH, pH 9.3−10.7; (e) Na_2HPO_4−NaOH, pH 10.9−11.5.[19] The percentages of sulfuric acid solution [(1 to 98) % H_2SO_4] were determined by titration with a primary standard substance Na_2CO_3 using methyl red as an indicator.[20] All of these materials and standard buffer solutions were from Merck and were not further purified.

Equipment. The pH values were measured by pH meter (pH/ion analyzer Orion 720 A+) furnished with a combined glass electrode. It was standardized at 25 °C by using standard buffers and calibrating at three points. To calibrate the pH meter, standard buffer solutions of pH 4.0, 7.0, and 9.0 were used. The UV−vis spectra, were recorded at each pH using a Hitachi 150-20 double beam spectrophotometer controlled by a computer and equipped with a 1 cm path length (quartz cells were used). All measurements were carried out at (25 ± 0.1) °C. The theoretical calculations were carried out using the Gaussian 03W program which is implemented in Intel based PCs.

10.1021/je100530r
Published on Web 11/29/2010

Procedures

Procedure for Spectrophotometric Measurement. The spectroscopic method depends on the direct determination of the ratio of the molecular species in a series of nonabsorbing buffer solutions for which pH values are either known or measured. To provide a series of buffers in highly acid regions, acidity functions H_o were used. Thus, for determining the acid dissociation constant of a very weak base, solutions of known H_o take the place of the buffer solutions mentioned above. For the protonation of the anion of a strong acid, which yields a neutral molecule, the function H_- was used. For a weak base B which ionizes by simple proton addition, the H_o, H_-, or pH values at half-protonations were measured for several compounds during the course of the present work, using the UV spectrophotometric method of Johnson.[21] This method takes into account any medium effect on the wavelength of the maximum UV absorption and the corresponding extinction coefficient. This effect is particularly significant at high acidities.

Bronsted (1923) was the first to show the advantage of having the ionization of both acids and bases (i.e., conjugate acids) expressed on the same scale, just as pH is used for basicity as well as for acidity. For acids the ionization process (i.e., deprotonation) is

$$HA \rightleftharpoons H^+ + A^- \quad (1)$$

and the ionization constant, K_a, is given by

$$K_a = \frac{[H^+][A^-]}{[HA]} \quad (2)$$

where [ ] represent the activity of each ionic species (in $mol \cdot L^{-1}$).

For bases the ionization is

$$BH^+ \rightleftharpoons B + H^+ \quad (3)$$

and

$$K_a = \frac{[B][H^+]}{[BH^+]} \quad (4)$$

At a given temperature, the constants expressed by eqs 2 and 4 are thermodynamic quantities also known as thermodynamic ionization constants. The equilibrium constants might be expressed in terms of concentration and activity coefficient (eq 5)[22]

$$K_a = \frac{[B][H^+]}{[BH^+]}\frac{\gamma_B\gamma_{H^+}}{\gamma_{BH^+}} \quad (5)$$

Therefore, the pK_a value can be expressed as follows (eq 6):

$$pK_a = pH + \log\frac{[BH^+]}{[B]} \quad (6)$$

pH Scale. A stock solution of 3AC (0.001 M) was prepared in an ethanol−water (1:1) mixed solvent. Sample solutions were prepared by adding 0.5 mL of stock solution to 9.5 mL of buffer solution and a sample solution series of 10 mL volumetric flasks were obtained. In this way, the sample solutions which have absorbance values of the UV−vis spectrum between 0.5−1.0 absorbance were prepared. All the series of standard solutions were placed in UV cells, hermetically closed and thermostatted at (25 ± 0.1) °C for 15 min. The UV−vis spectra were then recorded on the spectrophotometer within the range of (240 to 410) nm (1 nm resolution) (Figure 2). Simultaneously, the corresponding absorbance values were measured at three wavelengths of (272, 334, and 378) nm. Considerable changes were observed in the range of pH 9.08−11.20.

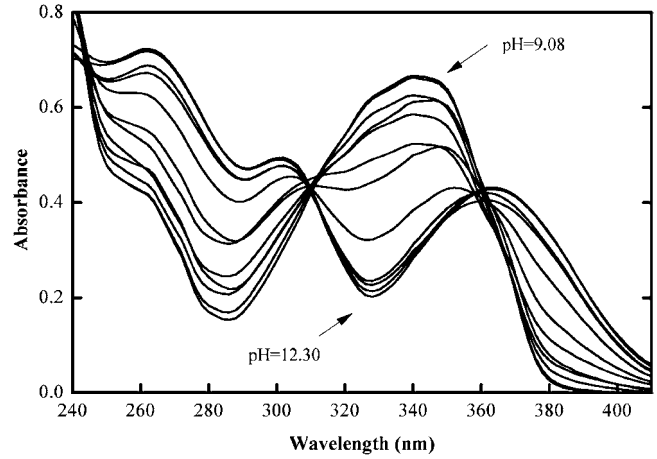

Figure 2. Spectral changes for the 3AC molecule at various pH conditions.

H_o Scale. The general procedure applied as follows; a stock solution of the compound under investigation was prepared by dissolving the compound (about (10 to 20) mg) in water or sulfuric acid of known strength (25 mL) in a volumetric flask. Aliquots (1 mL) of this solution were transferred into 10 mL volumetric flasks and diluted to the mark with sulfuric acid solutions of various strengths or buffers of various pH.[23] The total mass of solution in each flask was measured and the mass percent of sulfuric acid in each solution was then calculated knowing the mass of sulfuric acid added and the total mass of the final solution. In the case of buffer solutions, the pH was measured before and after addition of the new solution.[24] The absorbance of each solution was then measured in 1.0 cm cells, against solvent blanks, using a constant temperature cell-holder in a Hitachi 150-20 double beam spectrophotometer. The scanning spectrophotometer was thermostatted at (25 ± 0.1) °C. The wavelengths were chosen such that the fully protonated form of the substrate had a very much greater or very much smaller extinction coefficient than the neutral form. Calculations of half protonation values were carried out as follows; the sigmoid curve of absorbance or extinction coefficients at the analytical wavelength (A, λ) was first obtained (Figure 3). Since the deprotonation (ion formation) and protonation (cation formation) processes are both an equilibrium process we will give only one example for deprotonation.

The absorbance of the fully deprotonated molecule (A_{ca}; absorbance of conjugated base (anion)) and the pure free base (A_{fb}; absorbance of free base (neutral molecule)) at a basicity were then calculated by linear extrapolation of the arms of the curve. Equation 7 gives the ionization ratio where A_{obs} (the observed absorbance) was converted into the molar extinction coefficient ε_{obs} using Beers law of $A = \varepsilon bc$, (b = cell width, cm; c = concentration, $mol \cdot dm^{-3}$).

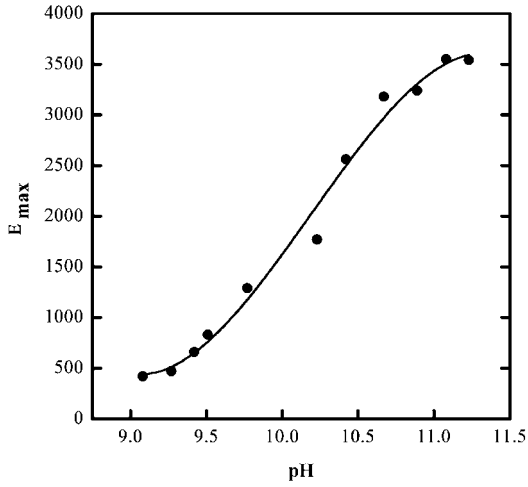

Figure 3. ε_{max} as a function of pH at (378 nm) plot for the deprotonation of 3AC.

$$I = \frac{[B]}{[BH^+]} = \frac{(A_{fb} - A_{obs})}{(A_{obs} - A_{ca})} = \frac{(\varepsilon_{fb} - \varepsilon_{obs})}{(\varepsilon_{obs} - \varepsilon_{ca})} \qquad (7)$$

A linear plot of log I against H_x or pH gives rise to a line in one form of $y = mx + n$, and by using the values $-1.0 < \log I < 1.0$, the slope, m, was obtained using the half protonation value as $H_x^{1/2}$ or $pH^{1/2}$ at $\log I = 0$; the pK_a values were obtained (Figure 4).[23]

The pK_a values were calculated by using the equation:

$$pK = mH_x^{1/2} \text{ (or } pH^{1/2}) \qquad (8)$$

When the values of the slope obtained m are around unity, then the base is called a Hammett base.[25]

Computational Methods

HF and DFT Calculations. We have used several theoretical methods and conclusively identified density functional theory (DFT) and the Hartree−Fock (HF) approach for ^{1}H and ^{13}C NMR chemical shifts as the most appropriate. The gauge including atomic orbital (GIAO) method, using the HF and DFT levels of theory with different basis sets were applied to the 3AC molecule. A detailed justification for the correlation of quantum mechanically calculated ^{1}H and ^{13}C NMR absolute chemical shielding tensors and empirical ^{1}H and ^{13}C NMR chemical shifts measured relative to tetramethylsilane (TMS) has also been presented.

Energies and frequencies of 3AC anions/cations were calculated using DFT, which has been a reliable technique for calculation of molecular properties and energetics. The initial geometries of the molecules were modeled by the DFT calculations included in the program CS Chem3D.[26] These geometries were optimized with the Gaussian 03W program packages,[27] using the B3LYP function with the 6-31G* basis set and the default convergence criteria. To analyze the solvent effects on all of the species involved in the proposed ionization reactions, the conductor-like polarizable continuum model (CPCM) was used.[28]

The B3LYP/6-31G* method reproduced very similar data, and this method is seen to be successful to describe the true value when the experimental values were taken as reference. A correlation between computed and experimental values was observed. As was indicated earlier, an excellent correlation between experimental and B3LYP/6-31G(d) calculated pK_a values (i.e., R^2 value is 0.995) was observed.

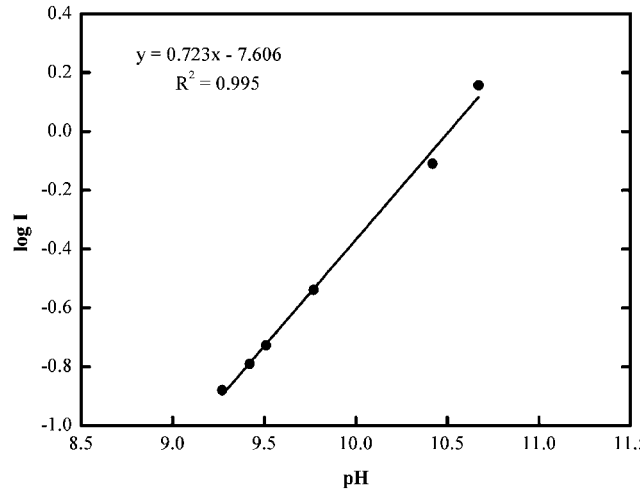

Figure 4. pH as a function of log I (at 378 nm), plot for the deprotonation of 3AC.

Scheme 1. Interrelationship between the Gas Phase and the Solution Phase Thermodynamic Parameters

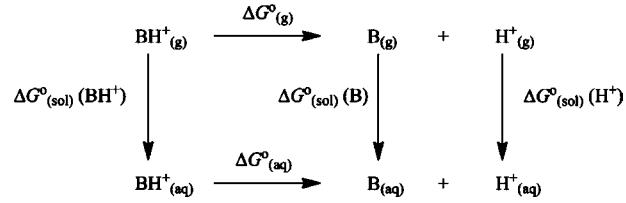

On the other hand, the experimental and the theoretical investigations of the 3AC molecule have been performed successfully by using NMR and quantum chemical calculations. Application of the GIAO method yields ^{1}H and ^{13}C NMR chemical shifts that are in reasonable agreement with experimental chemical shifts. The geometry of 3AC has been optimized using the 6-31G(d), 6-31+G(d), 6-31G(d,p), 6-311++G(d,p), and 6-311+G(d,p) basis sets. After optimization, ^{1}H and ^{13}C NMR chemical shifts (δ) were calculated for 3AC using the GIAO method with the B3LYP/6-31G(d), B3LYP/6-31G(d,p), B3LYP/6-311+G(2d,p), B3LYP/6-311+G(2d,2p), B3LYP/6-31+G(d,p), B3LYP/6-311+G(d,p), B3LYP/6-311++G(d,p), B3LYP/6-311++G(2d,p), and B3LYP/6-311++G(2d,p) basis sets and the Hartree−Fock method with the same basis sets. Relative chemical shifts were then estimated by using the corresponding TMS shielding, calculated in advance at the same theoretical level as the reference. The NMR chemical shifts were computed with the Becke-3-Lee−Yang−Parr (B3LYP) and HF with different basis sets using the GIAO method and are given relative to that of TMS calculated at the same level of theory. The GIAO ^{1}H and ^{13}C chemical shifts provide a reasonable reproduction of the experimental data.

General Scheme to Compute Absolute pK_a Values

Thermodynamic Cycle. Several authors have developed approaches for the computational determination of pK_a which involve the use of a thermodynamic cycle relating pK_a to the gas-phase proton basicity via the solvation energies ($\Delta G^o_{(sol)}$) of the products and the reactants (Scheme 1).

The inter- and intramolecular interactions can cause substantial changes in the geometry and electronic structure of compounds in solution in comparison with the isolated gas

Scheme 2. Possible Tautomeric, Protonation, and Deprotonation Patterns for 3AC

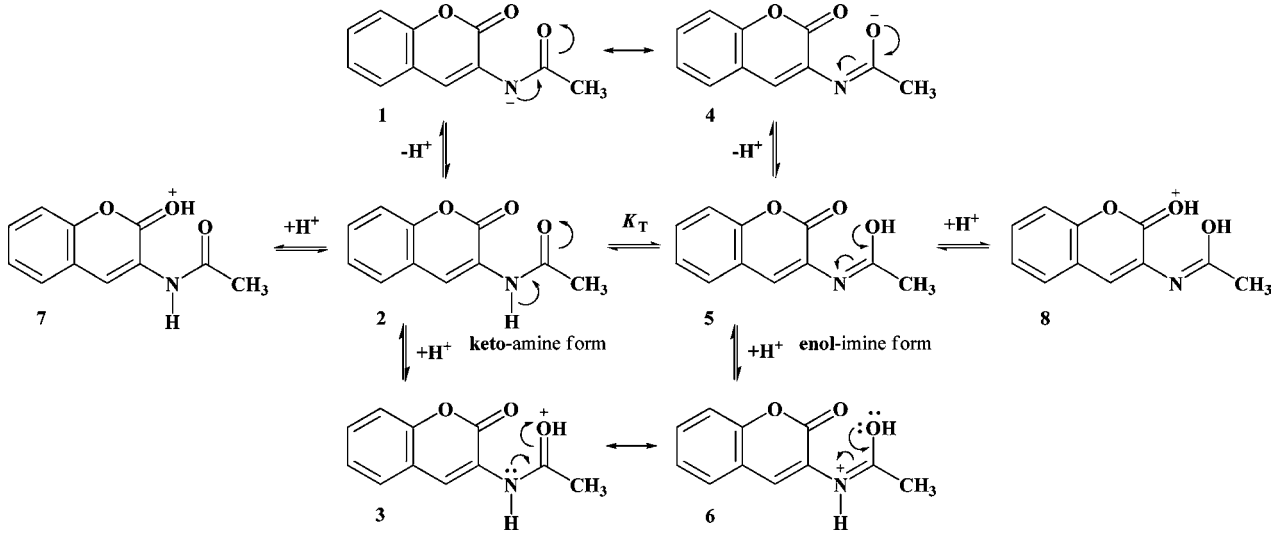

Table 1. Calculated Free Energies, G_g and G_{aq}, using Density Functional Theory (B3LYP/6-31G*)[a]

process	Gibbs energy (gas phase)		Gibbs energy (aqueous phase)		solvation Gibbs energy[b] (CPCM)	
protonation B + H^+ ⇌ BH^+	$G_{(g)}$(B)	$G_{(g)}$(BH^+)	$G_{(aq)}$(B)	$G_{(aq)}$(BH^+)	$\Delta G^o_{(sol)}$(B)	$\Delta G^o_{(sol)}$(BH^+)
2 ⇌ 3	−2949.37133	−2950.69296	−2949.37130	−2951.13626	0.01838031	278.176951
2 ⇌ 7	−2949.37133	−2950.77771	−2949.37130	−2951.11602	0.01838031	212.295285
5 ⇌ 6	−2949.23773	−2950.72446	−2949.29099	−2951.13235	−33.4199845	255.952095
5 ⇌ 8	−2949.23773	−2950.68682	−2949.29099	−2951.04523	−33.4199845	224.905560
deprotonation BH^+ ⇌ B + H^+	$G_{(g)}$(BH^+)	$G_{(g)}$(B)	$G_{(aq)}$(BH^+)	$G_{(aq)}$(B)	$\Delta G^o_{(sol)}$(BH^+)	$\Delta G^o_{(sol)}$(B)
2 ⇌ 1	−2949.37133	−2946.96158	−2949.37130	−2947.34252	0.01838031	−239.043844
5 ⇌ 4	−2949.23773	−2946.99718	−2949.29099	−2947.36021	−33.4199845	−227.809344

[a] All values are given in atomic unit, Hartree (1 hartree =2625.5 kJ·mol^{-1}). [b] Solvation energies calculated with CPCM and performed in Gaussian 03W.

phase. Therefore, the aqueous phase calculations are essential for pK_a determination and for this reason the CPCM solvation methods have been included in the present calculations. Calculation of the pK_a of a molecule, B, involves quantum mechanical calculations to characterize the gas phase system $\Delta G^o_{(g)}$ for both the associated acid, BH^+ (g), and the dissociated species, B (g) and H^+ (g), and to characterize the solvated system ($\Delta G^o_{(aq)}$) for the associated [BH^+ (aq)] and dissociated [B (aq) and H^+ (aq)] species. Thus, the pK_a of B (aq) is given by

$$pK_a = \Delta G^o_{(aq)}/2.303RT \quad (9)$$

$$pK_a = \frac{1}{2.303RT}(\Delta G^o_{(g)} - \Delta G^o_{(sol)}(BH^+) + \Delta G^o_{(sol)}(B) + \Delta G^o_{(sol)}(H^+)) \quad (10)$$

where

$$\Delta G^o_{(g)} = \Delta G^o_{(g)}(B) - \Delta G^o_{(g)}(BH^+) + \Delta G^o_{(g)}(H^+) \quad (11)$$

Most of the terms in this equation will be taken from our computations, but there are two terms that need careful consideration, the free energy of a proton in the gaseous phase $\Delta G^o_{(g)}(H^+)$ and its solvation free energy $\Delta G^o_{(sol)}(H^+)$. In the case of the free energy of a proton in the gaseous phase, it can be easily calculated by the Sackur−Tetrode equation[29]

$$\Delta G^o_{(g)}(H^+) = 2.5RT - T\Delta S = -26.28 \text{kJ·mol}^{-1} \quad (12)$$

Regardless of which procedure is used for absolute pK_a computation, knowledge of the proton solvation energy $\Delta G^o_{(sol)}(H^+)$ is required. For $\Delta G^o_{(g)}(H^+)$ the experimental value of −26.28 kJ·mol^{-1} is used. In the current work, we have used the values $\Delta G^o_{(g)}(H^+)$ = −26.28 kJ·mol^{-1} and $\Delta G^o_{(sol)}(H^+)$ = −1129.68 kJ·mol^{-1}.[30] The calculation of $\Delta G^o_{(g)}$ uses a reference state of 1 atm and the calculation of $\Delta G^o_{(sol)}$ uses a 1 M reference state. Converting the $\Delta G^o_{(g)}$ reference state (24.46 L at 298.15 K) from 1 atm to 1 M is accomplished. The absence of imaginary frequencies verified that all structures were true minima at their respective levels of calculation.

Tautomerism. Possible tautomerisation along with protonation and deprotonation patterns for the studied molecules are depicted in Scheme 2.

The tautomeric equilibrium constants were calculated from the Charlton method and the following equation[31] (eq 13) presented below:

$$pK_T = pK_{a(\text{model for product})} - pK_{a(\text{model for reactant})} \quad (13)$$

In this approach, the pK_a values of model molecules of both keto and enol forms are used. In models of the main tautomers the possibility of proton migrations were eliminated by replacing the acidic protons with methyl groups. All geometries were taken as starting points using B3LYP/6-31G(d) geometry optimiza-

Table 2. pK_a (= Half Protonation) Values of Protonation and Deprotonation Processes

process	pK_a (calc.)[a]	pK_a (expt.)
	Protonation	
2 ⇌ 7	−0.98	−0.74
2 ⇌ 3	−0.73	−0.74
5 ⇌ 6	16.23	−0.74
5 ⇌ 8	−0.24	−0.74
	Deprotonation	
2 ⇌ 1	18.23	10.16
5 ⇌ 4	10.17	10.16

[a] Calculated from eq 9.

Table 3. Isomerization K_i[a] and Tautomerization K_T[b] Constants for the Studied Molecule (DFT/6-31G*)

process	K_i[a] isomerization	K_T[b] tautomerization
1 ⇌ 4	$10^{8.06}$	
2 ⇌ 5		1.2×10^{-17}

[a] K_i values calculated by using $K_i = K_a$(enol form)/pK_a (keto form). [b] K_T values calculated by using $K_T = K_a$(enol form)/pK_a (keto form).

tions. The optimized structures were then used in the solution phase to determine the free energies (Table 1).

Results and Discussion

The spectra of 3AC are shown in Figure 3 for the pH values 9.08 and 12.30. The spectrum obtained at pH 1.16 (neutral 3AC) did not suffer modifications with a change of the pH of the reaction medium up to pH 6.48. On the other hand, considerable changes were observed in the range of pH 6.48 to 12.3. The spectrum obtained at pH 1.16 is practically identical to that of pH 6.48.

Evaluation of Acidity Constants and Tautomeric Equilibria. The computed thermodynamic energies and other physical parameters were obtained. The ab initio computed Gibbs energies ΔG, solvation energies ΔG_{sol}, and calculated and experimental acidity constant, pK_a, values are given in Tables 1 and 2.

A good correlation is observed between theoretical (ab initio) and the experimental values of the pK_a in the case of protonation (i.e., 2 ⇌ 3 equilibrium). So we can safely state that the molecule exists in the keto-amine form **2** before protonation and protonates at the acetamide carbonyl group. With the same analogy we can say that the molecule exists in the enol-imine form **5** before deprotonation and deprotonation occurs therefore at the −OH group of acetamide (i.e., 5 ⇌ 4 equilibrium) (Table 2). Similarly the values of the tautomeric equilibrium constant, K_T, and isomerization constant, K_i, can be evaluated (Table 3). The K_i value of $10^{8.06}$ for the isomerization equilibrium 1 ⇌ 4 indicates the predominance of the enolate form **4** over the enamine form **1** with a ratio of 4:1 = 114.82. The value of 1.2×10^{-17} for tautomerization for 2⇌5 indicates the overwhelming predominance of the keto-amino form **2** over the enol-imine form **5**.

GIAO Predictions of ^{1}H/^{13}C Chemical Shifts and Comparison with Experimental Results. The GIAO method with the B3LYP function of theory and Hartree−Fock theory was employed to interpret available NMR data (chemical shifts) of 3AC. The calculations are summarized in Table 4 (bold characters in Table 4 show the best fit to experimental data).

The depicted list of GIAO theoretical isotropic ^{1}H and ^{13}C NMR chemical shifts relative to TMS are obtained with the Hartree−Fock and DFT for 3AC. Various different approaches

Table 4. ^{1}H and ^{13}C NMR Experimental[a] Chemical Shifts and Calculated Absolute Shieldings (δ, ppm)

		^{1}H NMR							^{13}C NMR									
	basis sets/methods	H(1−2−3)	H4	H5	H6	H7	H8	H9	C1	C2	C3	C4	C5	C6	C7	C8	C9	C10	C11
1	B3LYP/6-31G(d)//B3LYP/6-31G(d)	**1.58**	**7.68**	**8.17**	**6.90**	**6.83**	**6.96**	**6.74**	16.07	150.69	113.02	142.15	136.83	103.10	114.84	110.72	114.50	108.43	108.73
2	B3LYP/6-31G(d,p)//B3LYP/6-31G(d,p)	2.06	8.05	9.07	7.53	7.43	7.57	7.42	14.33	150.69	113.25	142.16	136.91	102.39	114.11	110.03	113.85	108.56	108.08
3	B3LYP/6-311+G(2d,p)//B3LYP/6-31G(d)	2.09	8.27	9.35	7.71	7.56	7.69	7.58	24.51	173.82	131.22	164.47	159.13	121.20	133.96	129.51	133.97	127.60	127.50
4	B3LYP/6-311+G(2d,2p)//B3LYP/6-31G(d)	2.32	8.70	9.59	7.92	7.74	7.88	7.78	24.81	173.90	131.28	164.59	158.99	121.45	134.05	129.49	134.03	127.57	127.34
5	B3LYP/6-31+G(d,p)//B3LYP/6-31+G(d)	2.50	8.42	7.04	7.59	7.66	7.80	7.77	16.27	152.78	114.32	143.61	137.96	104.03	114.84	110.98	113.18	109.37	102.79
6	B3LYP/6-311+G(d,p)//B3LYP/6-31+G(d)	2.29	8.10	7.04	7.42	7.44	7.54	7.53	26.37	172.51	131.58	162.73	157.71	121.81	133.97	129.89	130.91	126.10	118.66
7	B3LYP/6-311++G(d,p)//B3LYP/6-311++G(d,p)	2.18	7.77	6.92	7.34	7.33	7.50	7.46	24.97	170.91	131.09	160.97	157.13	121.2	133.22	128.88	130.00	125.06	119.57
8	B3LYP/6-311++G(2d,p)//B3LYP/6-311++G(d,p)	2.27	7.95	7.15	7.50	7.46	7.61	7.54	25.42	172.01	132.19	162.42	157.88	120.94	133.24	128.90	130.34	126.26	120.59
9	B3LYP/6-311+G(d,p)//B3LYP/6-311+G(d,p)	1.95	7.82	9.05	7.50	7.36	7.48	7.43	23.79	172.16	129.75	161.67	157.74	120.69	133.43	128.78	132.04	125.82	126.13
10	**B3LYP/6-311++G(2d,p)//B3LYP/6-311+G(d,p)**	2.26	7.96	7.13	7.49	7.47	7.62	7.54	**25.58**	**171.98**	**132.20**	**162.20**	**157.71**	**126.24**	**133.27**	**128.91**	**130.35**	**126.24**	**120.59**
11	HF/6-31G(d)//HF/6-31G(d)	1.69	6.12	8.29	7.42	7.16	7.43	7.24	21.87	162.22	120.43	151.46	143.33	113.07	127.24	119.72	127.29	114.33	118.89
12	**HF/6-31G(d,p)//HF/6-31G(d,p)**	2.13	7.19	9.05	8.04	7.77	7.02	7.91	**20.45**	**162.40**	**120.70**	**151.63**	**143.48**	**112.56**	**126.84**	**119.29**	**125.50**	**114.52**	**118.37**
13	**HF/6-311+G(2d,p)//HF/6-31G(d)**	**2.22**	**7.29**	**9.14**	**8.09**	**7.75**	**8.01**	**7.89**	29.53	179.91	134.07	168.51	160.09	126.62	141.73	133.80	139.64	128.83	133.27
14	HF/6-311+G(2d,2p)//HF/6-31G(d)	2.48	7.17	7.67	8.21	7.99	8.32	8.18	27.31	180.33	136.73	136.71	161.20	127.53	143.42	134.05	138.73	127.41	135.62
15	HF/6-31+G(d,p)//HF/6-31+G(d)	2.38	6.96	7.53	8.10	7.89	8.19	8.15	18.42	163.94	122.22	151.05	145.26	113.36	128.40	119.27	124.25	113.85	121.09
16	HF/6-311+G(d,p)//HF/6-31+G(d)	2.19	6.65	7.28	7.87	7.68	8.00	7.94	26.78	179.01	135.54	165.99	160.41	127.80	143.25	134.08	138.47	126.51	134.54
17	HF/6-311++G(d,p)//HF/6-311++G(d,p)	2.17	6.46	7.28	7.85	7.64	7.97	7.91	26.69	177.44	135.29	164.38	160.19	127.38	142.75	133.53	137.97	125.97	134.79
18	HF/6-311++G(2d,p)//HF/6-311++G(d,p)	2.25	6.56	7.43	7.93	8.07	7.74	7.96	27.59	178.54	136.48	165.83	160.80	127.06	142.89	133.51	138.30	126.87	135.77
19	HF/6-311+G(d,p)//HF/6-311+G(d,p)	2.17	6.45	7.26	7.84	7.64	7.98	7.90	26.55	177.24	135.31	164.4	160.11	127.40	142.71	133.53	138.10	125.95	134.85
20	HF/6-311++G(2d,p)//HF/6-311+G(d,p)	2.24	6.56	7.42	7.96	7.74	8.07	7.93	27.54	178.70	136.48	165.82	160.83	127.06	142.86	133.51	138.31	126.87	135.75
	experimental	2.18	8.17	8.68	7.50	7.30	7.44	7.30	27.72	169.42	149.80	158.69	119.79	123.22	129.56	127.75	125.11	123.97	116.27

[a] Experimental data taken from ref 33.

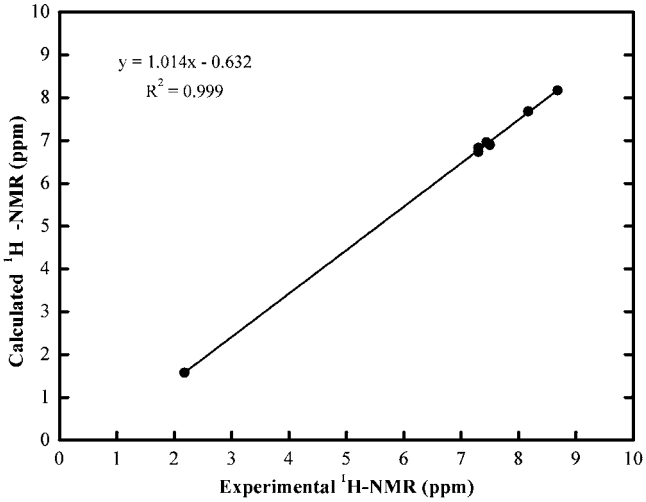

Figure 5. Comparison of experimental and theoretical ^{1}H NMR chemical shifts for 3AC (calculated at the B3LYP/6-31G(d)//B3LYP/6-31G(d) level of the theory).

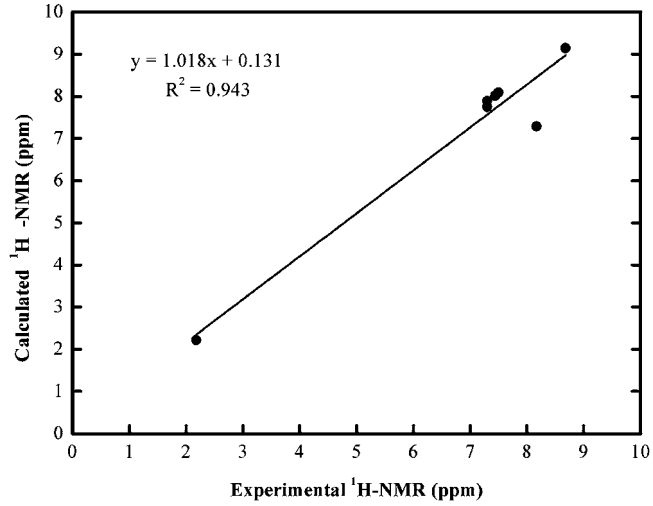

Figure 6. Comparison of experimental and theoretical ^{1}H NMR chemical shifts of 3AC (calculated at the HF/6-311+G(2d,p)//HF/6-31G(d) level of the theory).

have been developed and tested, however, the most widely used technique is the GIAO calculation of ^{1}H and ^{13}C NMR chemical shifts at the DFT B3LYP 6-311++G(2d,p) level which is suitable for organic molecules.

All of the structures were fully optimized with the Gaussian 03W program with the B3LYP and HF methods with different basis sets. After the optimization, ^{1}H and ^{13}C NMR chemical shifts were calculated with the GIAO method using corresponding TMS shielding calculated at the same theoretical level as the reference. However, prediction of ^{1}H and ^{13}C NMR chemical shifts using any of the methods is in good agreement with experiment.[32] In order to compare isotropic shielding with experimental chemical shifts, the NMR parameters for TMS were calculated for each basis set and used as the reference molecule.

The data in Table 4 reveal that the Hartree−Fock based calculation results are in excellent agreement with the experimental^{13}C chemical shift data. The B3LYP-based calculation demonstrates similar agreement for the^{1}H chemical shifts. The GIAO calculations were performed using DFT (B3LYP) with the 6-31G(d), 6-31G(d,p), 6-31+G(d,p), 6-311+G(d,p), 6-311++G(d,p), 6-311+G(2d,p), 6-311++G(2d,p), and 6-311+G(2d,2p) basis set as recommended[33] and Hartree−Fock levels of theory with the same basis sets. These trends are in good agreement with experimental results.

Although linear correlations typically exist between experimental and theoretical values predicted in this manner, the slope of the line can deviate from unity, depending on the computational method and choice of basis set (Figures 5, 6, 7, and 8).[34] The deviation from linearity for some points obviously occurs due to the presence of the N−H and O−H groups which can easily form hydrogen bonding. Another possibility of course is the medium effect on these groups.

A linear scaling of the calculated chemical shifts is used in order to account for the differences in the conditions of the experimental measurements and computational predictions, as well as for possible systematic errors either at the geometry optimization or NMR stages of the calculations.

Conclusion

In this study, the experimental and theoretical investigations of the 3AC molecule have been performed successfully by using NMR and quantum chemical calculations. First, we proved the

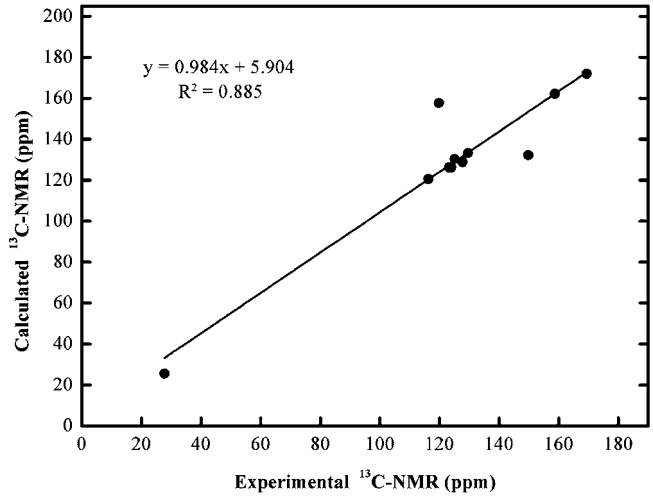

Figure 7. Comparison of experimental and theoretical ^{13}C NMR chemical shifts of 3AC (calculated at the B3LYP/6-311++G(2d,p)//B3LYP/6-311+G(d,p) level of the theory).

feasibility of a UV−vis spectroscopic method using the absorbance values to determine the ionization constants of 3AC in EtOH−water solutions. To analyze the solvent effects on all of the species involved in the proposed ionization reactions, the PCM of Tomasi and co-workers was used.[35] The calculations were performed at DFT/6-31G* using Tomasi's method. To calculate solvation energies, a popular continuum model of solvation has been used at the B3LYP levels of theory in conjunction with the 6-31G* basis set. The theoretically obtained protonation and deprotonation constants exhibit good agreement with the acidity constants which were experimentally determined in our present work. A reasonable correlation was obtained between the protonation/deprotonation energies of the compounds calculated at the B3LYP/6-31G* levels of theory and their aqueous pK_a values. Ability to predict acidity using a coherent, well-defined theoretical approach, without external approximation or fitting to experimental data would be very useful to chemists. Finally, it seems that theoretical calculations of physical parameters provide satisfactory results to supplement experimental findings for quantitative structure−activity relation studies.

We also now report a unique collection of experimental NMR data (chemical shifts) for 3AC showing the effectiveness of

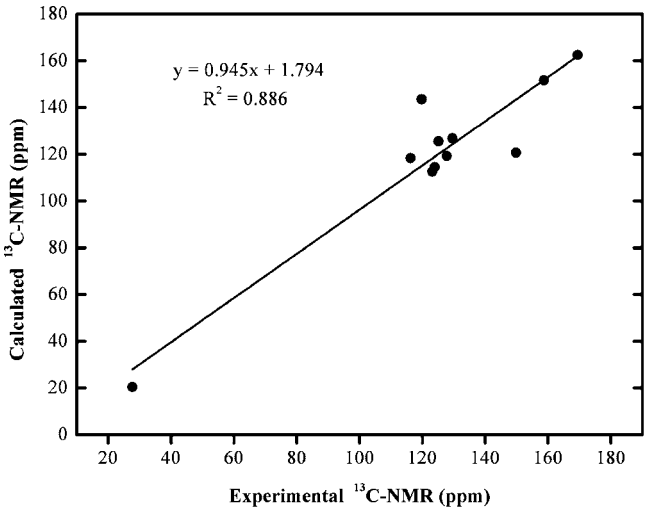

Figure 8. Comparison of experimental and theoretical ^{13}C NMR chemical shifts of 3AC (calculated at the HF/6-31G(d,p)//HF/6-31G(d,p) level of the theory).

GIAO/DFT and GIAO/HF calculations in predicting chemical shifts. NMR methods are a very powerful tool for the study of molecular behavior in heterogeneous systems.[36] Some difficulties that arise in the interpretation of the origin of certain NMR signals can be overcome by quantum chemistry calculations. In this part of our study, the GIAO methods using the B3LYP and HF with different basis sets were applied to 3AC. Application of the GIAO method yields ^{1}H and ^{13}C NMR chemical shifts that are in agreement with experimental results. Comparison of the B3LYP and HF methods showed that the best results for small molecules with the HF/HF approach. For the ^{13}C shieldings, the HF/HF calculations were almost identical in quality and for ^{1}H NMR the B3LYP/B3LYP performed better. The GIAO/DFT approach predicted the ^{13}C NMR shifts of heteroaromatic ring carbons which are in better agreement with experiment. To summarize our results, we report a general correlation between experimental and theoretical results for ^{1}H and ^{13}C NMR and pK_a data. The calculated isotropic shielding constants based on DFT/GIAO and HF/GIAO methods are found to be in good agreement with the experimental results.

Acceptable agreements between the theoretical and experimental results were observed for the HF level ^{13}C NMR chemical shifts and for the B3LYP-type ^{1}H NMR chemical shifts.

Acknowledgment

Our research group is greatly in debt to the Board of Scientific Research Projects of Eskişehir Osmangazi University for providing the Gaussian 03W program.

Literature Cited

(1) Kudale, A. A.; Kendall, J.; Warford, C. C.; Wilkins, D. N.; Bodwell, G. J. Hydrolysis-Free Synthesis of 3-Aminocoumarins. *Tetrahedron Lett.* **2007**, *48*, 5077–5080.

(2) Bultink, I. E. M.; Lems, W. F.; Kostense, P. J.; Dijkmans, B. A. C.; Voskuyl, A. E. Prevalence of and Risk Factors for Low Bone Mineral Density and Vertebral Fractures in Patients with Systemic Lupus Erythematosus. *Arthritis Rheum.* **2005**, *52*, 20–44.

(3) O'Reilly, R. A. Vascular and Lymphatic Absorption of Radioactive Albumin From The Lungs. *J. Clinic. Investig.* **1967**, *46*, 829–835.

(4) Zhao, H.; Neamati, N.; Hong, H.; Mazumder, A.; Wang, S.; Sunder, S.; Milne, G. W. A.; Pommier, Y.; Burke, T. R. Coumarin-Based Inhibitors of HIV Integrase. *J. Med. Chem.* **1997**, *40*, 242–249.

(5) Hirsh, J.; Dalen, J. E.; Anderson, D. R.; Poller, L.; Bussey, H.; Ansell, J.; Deykin, D. Oral Anticoagulants: Mechanism of Action, Clinical Effectiveness, and Optimal Therapeutic Range. *Chest* **2001**, *119*, 8–21.

(6) Kashman, Y.; Gustafson, K. R.; Fuller, R. W.; Cardellina, J. H.; McMahon, J. B.; Currens, M. J.; Buckheit, R. W.; Hughes, S. H.; Cragg, G. M.; Boyd, M. R. HIV Inhibitory Natural Products. The Calanolides, a Novel HIV-Inhibitory Class of Coumarin Derivatives from the Tropical Rainforest Tree, Calophyllum Lanigerum. *J. Med. Chem.* **1992**, *35*, 2735–2740.

(7) Fylaktakidou, K. C.; Hadjipavlou-Litina, D. J.; Litinas, K. E.; Nicolaides, D. N. Natural and Synthetic Coumarin Derivatives with Anti-inflammatory/Antioxidant Activities. *Curr. Pharm. Des.* **2004**, *10*, 3813–3833.

(8) Gacche, R. N.; Gond, D. S.; Dhole, N. A.; Dawane, B. S. Coumarin Schiff-bases: As Antioxidant and Possibly Anti-inflammatory Agents. *J. Enz. Inhib. Med. Chem.* **2006**, *21*, 157–160.

(9) Breda, S.; Lapinski, L.; Fausto, R.; Nowak, J. Photoisomerization Reactions of 4-Methoxy- and 4-Hydroxy-6-Methyl-α-Pyrones: An Experimental Matrix Isolation and Theoretical Density Functional Theory Study. *Phys. Chem. Chem. Phys.* **2003**, *5*, 4527–4532.

(10) Magill, A. M.; Yates, B. F. An Assessment of Theoretical Protocols for Calculation of the pK_a Values of the Prototype Imidazolium Cation. *Aust. J. Chem.* **2004**, *5*, 1205–1210.

(11) Van de Waterbeemd, H.; Gifford, E. ADMET in Silico Modelling: Towards Prediction Paradise. *Nat. Rev. Drug Discovery* **2003**, *2*, 192–204.

(12) Van de Waterbeemd, H.; Lennernäs, H.; Artursson, P. *Drug Bioavailability*; Wiley: Weinheim, Germany, 2004.

(13) Kunz, K. R.; Iyengar, B. S.; Dorr, R. T.; Alberts, D. S.; Remers, W. A. Structure-Activity Relationships for Mitomycin C and Mitomycin A Analogues. *J. Med. Chem.* **1991**, *34*, 2281–2286.

(14) Patrick, G. L. *Introduction to Medicinal Chemistry*; Oxford University Press: New York, 1995.

(15) Kaufman, J. J.; Semo, N. M.; Koski, W. S. Microelectrometric Titration Measurement of the pK_a's and Partition and Drug Distribution Coefficients of Narcotics and Narcotic Antagonists and their pH and Temperature Dependence. *J. Med. Chem.* **1975**, *18*, 647–655.

(16) Fleuren, H. L. J.; Van Ginneken, C. A. M.; Van Rossum, J. M. Differential Potentiometric Method for Determining Dissociation Constants of Very Slightly Water-Soluble Drugs Applied to the Sulfonamide Diuretic Chlorthalidone. *J. Pharm. Sci.* **1979**, *68*, 1056–1058.

(17) Lišková, A.; Křivánková, L. Determination of Dissociation Constants of Compounds with Potential Cognition Enhancing Activity by Capillary Zone Electrophoresis. *Electrophoresis* **2005**, *26*, 4429–4439.

(18) Öğretir, C.; Demirayak, Ş.; Duran, M. Spectroscopic Determination and Evaluation of Acidity Constants for Some Drug Precursor 2-Amino-4-(3- or 4-substituted phenyl) Thiazole Derivatives. *J. Chem. Eng. Data* **2010**, *55*, 1137–1142.

(19) Robinson, R. A.; Stokes, R. H. *Electrolyte solutions*; Butterworths, London, 1968.

(20) Sabnis, R. W. *Handbook of Acid-Base Indicators*; CRC Press, Boca Raton, FL, 2008.

(21) Johnson, C. D.; Katritzky, A. R.; Ridgewell, B. J.; Shakir, N.; White, A. M. The Applicability of Hammett Acidity Functions to Substituted Pyridines and Pyridines 1-oxides. *Tetrahedron* **1965**, *21*, 1055–1059.

(22) Cookson, R. F. The Determination of Acidity Constants. *Chem. Rev.* **1974**, *74*, 1–3.

(23) Albert, A.; Serjeant, E. P. *The Determination of Ionization Constants*; Chapman and Hall Ltd.: London, 1971.

(24) Schawarzenbach, G.; Sulzberger, R. The Alkalinity of Strong Solutions of the Alkali Hydroxides. *Helv. Chim. Acta* **1944**, *27*, 348–362.

(25) Sokolov, S. D.; Tikhomirova, G. B. Research in the Isoxazole Series. Basicities of Phenylisoxazoles. *Chem. of Hetero. Comp.* **1975**, *12*, 851–853.

(26) *Program CS Chem3D Ultra 10.0. Molecular Modeling and Analaysis*, Cambridge Soft Corporation: Cambridge, MA, 2006.

(27) Frisch, M. J.; Trucks, G. W.; Schlegel, H. B.; Scuseria, G. E.; Robb, M. A.; Cheeseman, J. R.; Montgomery, J. A., Jr.; Vreven, T.; Kudin, K. N.; Burant, J. C.; Millam, J. M.; Iyengar, S. S.; Tomasi, J.; Barone, V.; Mennucci, B.; Cossi, M.; Scalmani, G.; Rega, N.; Petersson, G. A.; Nakatsuji, H.; Hada, M.; Ehara, M.; Toyota, K.; Fukuda, R.; Hasegawa, J.; Ishida, M.; Nakajima, T.; Honda, Y.; Kitao, O.; Nakai, H.; Klene, M.; Li, X.; Knox, J. E.; Hratchian, H. P.; Cross, J. B.; Bakken, V.; Adamo, C.; Jaramillo, J.; Gomperts, R.; Stratmann, R. E.; Yazyev, O.; Austin, A. J.; Cammi, R.; Pomelli, C.; Ochterski, J. W.; Ayala, P. Y.; Morokuma, K.; Voth, G. A.; Salvador, P.; Dannenberg, J. J.; Zakrzewski, V. G.; Dapprich, S.; Daniels, A. D.; Strain, M. C.; Farkas, O.; Malick, D. K.; Rabuck, A. D.; Raghavachari, K.; Foresman, J. B.; Ortiz, J. V.; Cui, Q.; Baboul, A. G.; Clifford, S.; Cioslowski, J.; Stefanov, B. B.; Liu, G.; Liashenko, A.; Piskorz, P.; Komaromi, I.; Martin, R. L.; Fox, D. J.; Keith, T.; Al-Laham, M. A.; Peng, C. Y.;

Nanayakkara, A.; Challacombe, M.; Gill, P. M. W.; Johnson, B.; Chen, W.; Wong, M. W.; Gonzalez, C.; Pople, J. A. Gaussian 03; Gaussian, Inc.: Wallingford, CT, 2004.

(28) Barone, V.; Cossi, M. Quantum Calculation of Molecular Energies and Energy Gradients in Solution by a Conductor Solvent Model. *J. Phys. Chem. A* **1998**, *11*, 1995–2001.

(29) Wedler, G. *Lehrbuch der Physikalischen Chemie*; Verlag Chemie: Weinheim, Germany, 1982.

(30) Liptak, M. D.; Gross, K. C.; Seybold, P. G.; Feldgus, S.; Shields, G. C. Absolute pK_a Determinations for Substituted Phenols. *J. Am. Chem. Soc.* **2002**, *124*, 6421–6427.

(31) Katritzky, A. R.; Rees, C. W.; Scriven, E. F. V. *Comprehensive Heterocyclic Chemistry II*; Pergamon Press: Oxford, 1996.

(32) Pouchert, C. J.; Behnke, J. *The Aldrich Library of ^{13}C and ^{1}H FT NMR Spectra, 300 MHz ^{1}H/75 MHz^{13}*; Aldrich Chemical Co.: Milwaukee, WI, 1993.

(33) Urbelis, G.; Susvilo, I.; Tumkevicius, S. Investigation of the Structure of 6-Amino-4-Methylamino-5-Nitrosopyrimidine by X-ray Diffraction, NMR and Molecular Modeling. *J. Mol. Model.* **2007**, *13*, 219–224.

(34) Giesen, D. J.; Zumbulyadis, N. A. Hybrid Quantum Mechanical and Empirical Model for the Prediction of Isotropic 13C Shielding Constants of Organic Molecules. *J. Phys. Chem.* **2002**, *4*, 5498–5507.

(35) Blanco, S. E.; Almandoz, M. C.; Ferretti, F. H. Determination of the overlapping pK_a values of resorcinol using UV-visible spectroscopy and DFT methods. *Spectrochim. Acta, Part A* **2005**, *61*, 93–102.

(36) Wolinski, K.; Hinton, J. F.; Pulay, P. Efficient Implementation of the Gauge-Independent Atomic Orbital Method for NMR Chemical Shift Calculations. *J. Am. Chem. Soc.* **1990**, *112*, 8251–8260.

Received for review May 21, 2010. Accepted November 12, 2010.

JE100530R